Supporting Information

# Divanillin based polyazomethines: toward bio-based and metal-free π-conjugated polymers

Guillaume Garbay, †# [a] Lauriane Giraud,# [a] Sai Manoj Gali, [a] Georges Hadziioannou, [a] Etienne Grau,[a] Stéphane Grelier,[a] Eric Cloutet, [a] * Henri Cramail, [a] * Cyril Brochon [a] *

[a] Laboratoire de Chimie des Polymères Organiques (LCPO UMR 5629), CNRS-Université de Bordeaux-Bordeaux INP, 16 Avenue Pey-Berland, Pessac, 33607 Cedex, France

† current address : Arkema, Centre de production de Feuchy, BP 70029, 62051 Saint-Laurent-Blangy Cedex, France

**Table of contents**

## Computational Details

*1. Electronic and optical properties of monomers*

Relaxed potential energy surface scans were first performed on monomer units of **DV-Cbz** and **DV-Ph** to sample the possible stable conformations with respect to the torsional angles around single bonds. Calculations were performed at PBE0/6-31(d,p) level of theory with chloroform as implicit solvent using CPCM implicit solvation model. Three dihedral angles were considered for each derivative, $\theta_1$, $\theta_2$ and $\theta_3$ as shown in **Figure S15**. Corresponding energy scans are presented in **Figure S16**.

The relative energies ($\Delta E$ in kcal/mol) of the various stable conformers obtained from the Potential Energy Surface (PES) scans are collected in **Table S1**.

In a second step, **DV-Ph** and **DV-Cbz** derivatives were fully optimized by starting from the lowest-energy conformer obtained from the PES scans. Optimizations were carried out at the DFT level using the 6-31(d,p) basis set with various exchange-correlation functionals (XCFs) and chloroform as implicit solvent. Frequency calculations were then performed to ensure proper optimization of the geometries. **Table S2** reports the HOMO and LUMO energies (in eV), as well as the electronic band gap ($E_G = E_{LUMO} - E_{HOMO}$) of both derivatives, for a selection of exchange-correlation functionals (XCFs). Irrespective of the DFT functional employed, $E_{G-\mathbf{DV\text{-}Cbz}} < E_{G-\mathbf{DV\text{-}Ph}}$.

Furthermore, vertical transition energies ($E_{Vert}$) were computed at the time-dependent DFT (TD-DFT) level using the same XCFs and basis set as those employed in geometry optimizations. Consistently with the electronic band gap, results collected in **Table S2** also show that $E_{Vert-\mathbf{DV\text{-}Cbz}} < E_{Vert-\mathbf{DV\text{-}Ph}}$, irrespective of the choice of XCF selected.

*2. Electronic and optical properties of increasing-size oligomers*

Similar DFT and TD-DFT calculations were then carried out on increasing-size oligomers of both derivatives, using the B3LYP and CAM-B3LYP functionals. B3LYP was selected since it provides good estimate of the HOMO and LUMO energy levels compared to those deduced experimentally from cyclic voltammetry measurements, although such comparisons are highly approximate. CAM-B3LYP was selected because it is known to improve the description of low-lying charge-transfer excited states in push-pull dyes [S1]. Electronic band gaps ($E_G$) and vertical transition energies ($E_{Vert}$) as a function of chain length of the oligomers are gathered in **Table S3**. Irrespective of the increase in chain length, $E_{G-\mathbf{DV\text{-}Cbz}} < E_{G-\mathbf{DV\text{-}Ph}}$.

*3. Electronic and optical gaps at polymer limit*

Finally, the size-converged electronic and optical gaps were evaluated using a fitting procedure based on the Khun's model, which is based on linear coupling of double bonds (harmonic oscillators) that contribute to electronic transitions.[S2, S3] In this procedure, the electronic gap or vertical transition energies reported in **Table S3** are first plotted against 1/N, where N is the number of double bonds along the shortest conjugated pathway connecting the terminal carbon of the oligomers. Then, a linear regression can be obtained based on Khun's equation (Equation 1) to extract energy gaps at polymer limit:

$$E_g = E_0\sqrt{1 + D_k cos\left(\frac{\pi}{N+1}\right)} \quad (1)$$

In the above equation, $E_0$ and $D_k$ are the fitting parameters. $E_0$ corresponds to the energy gap when N = 1 and $D_k$ is a force constant that represents the strength of coupling between single and double bonds in a given oligomer, entailing that $D_k$ is implicitly linked to the efficiency of the π-conjugation between consecutive monomeric units (higher the value of $D_k$, higher the delocalization of π electrons).[S4]

The evolution of the electronic and optical gaps as a function of 1/*N*, calculated at the B3LYP/6-31G(d) and CAM-B3LYP/6-31G(d) levels, are shown in **Figure S17**. The size-converged electronic and optical gaps, as well as the optimized $E_0$ and $D_k$ parameters, are reported in **Table S4**. The two levels of calculation predict that the **DV-Cbz** derivative shows lower electronic and optical gaps at polymer limit than the **DV-Ph** derivative. This relative ordering both originates from a lower value of the band gap of the **DV-Cbz** monomer (see section 1), and from a more efficient π-conjugation between consecutive units, as indicated by the larger $D_k$ values.

*References*


**[S1]** Jacquemin, D.; Perpète, E. A.; Scuseria, G. E.; Ciofini, I. ; Adamo, C. TD-DFT Performance for the Visible Absorption Spectra of Organic Dyes: Conventional versus Long-Range Hybrids, *J. Chem. Theory Comput.*, **2008**, *4*, 1.

**[S2]** Gierschner, J.; Cornil, J.; Egelhaaf, H.-J. Optical Bandgaps of π‐Conjugated Organic Materials at the Polymer Limit: Experiment and Theory, *Advanced Materials*, **2007**, *19*, 173.

**[S3]** Torras, J.; Casanovas, J.; Alemn, C. Reviewing Extrapolation Procedures of the Electronic Properties on the π-Conjugated Polymer Limit, *The Journal of Physical Chemistry A*, **2012**, *116*, 7571.

**[S4]** Wykes, M.; Milin-Medina, B.; Gierschner, J. Computational engineering of low bandgap copolymers, *Frontiers in Chemistry*, **2013**, *1*, 35.

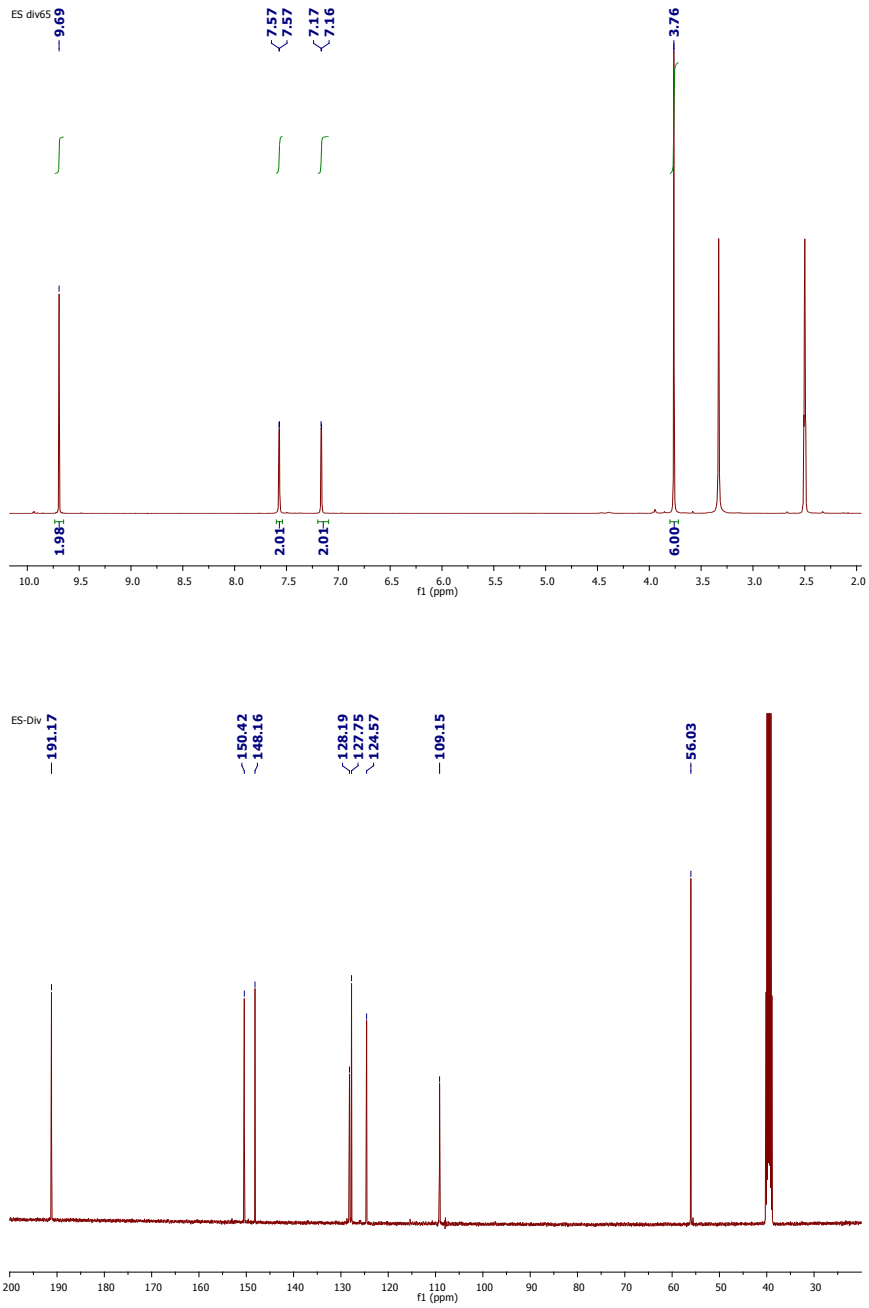


**Figure S1.** $^{1}$H-NMR (top) and $^{13}$C-NMR (bottom) spectra of **DV** (400.20 MHz and 100.63 MHz respectively, in $(CD_3)_2SO$)

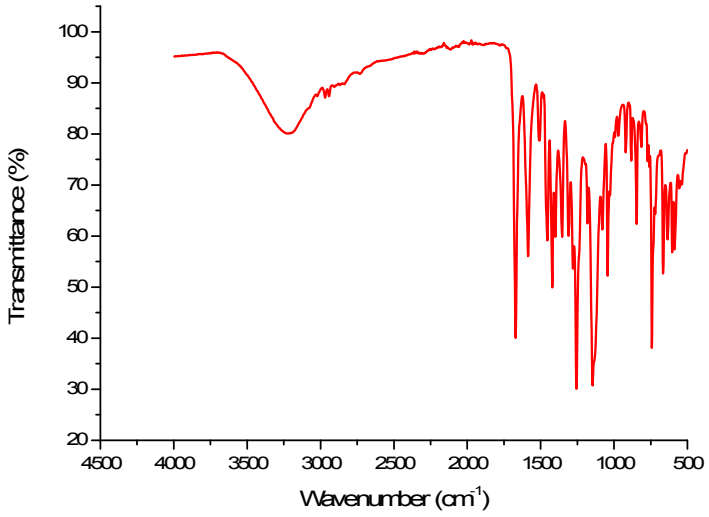


**Figure S2.** ATR-FTIR spectrum of **DV**

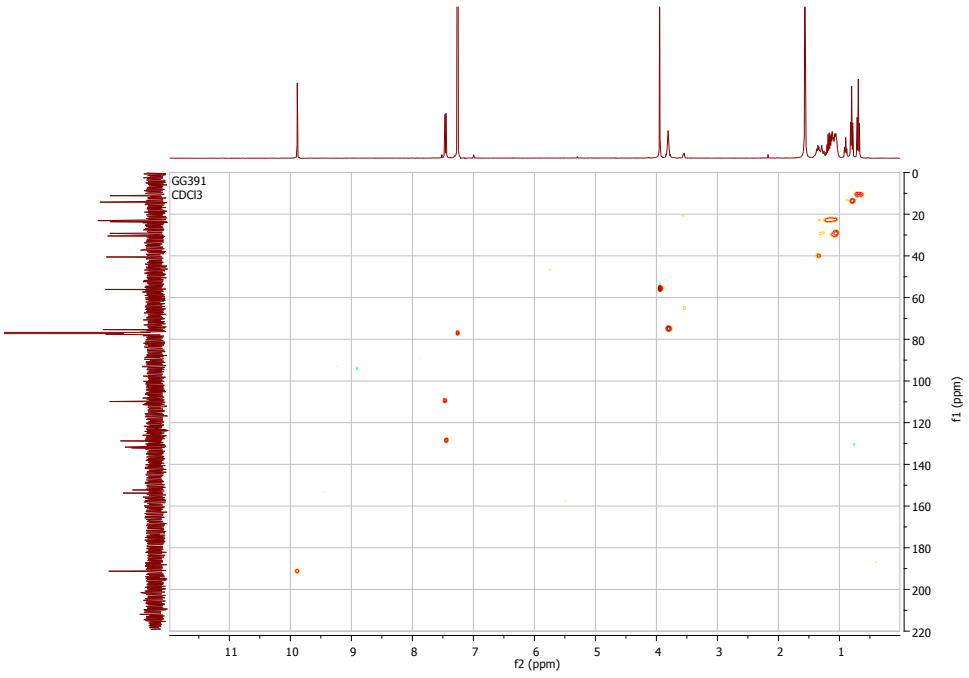


**Figure S3.** $^{1}H$-$^{13}C$ HSQC NMR spectrum of **DVEH** (400.20 MHz and 100.63 MHz respectively, in $CDCl_3$)

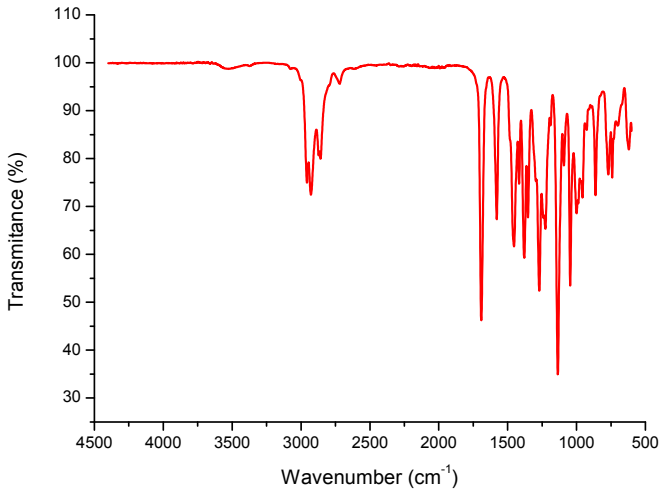


**Figure S4.** ATR-FTIR spectrum of **DVEH**

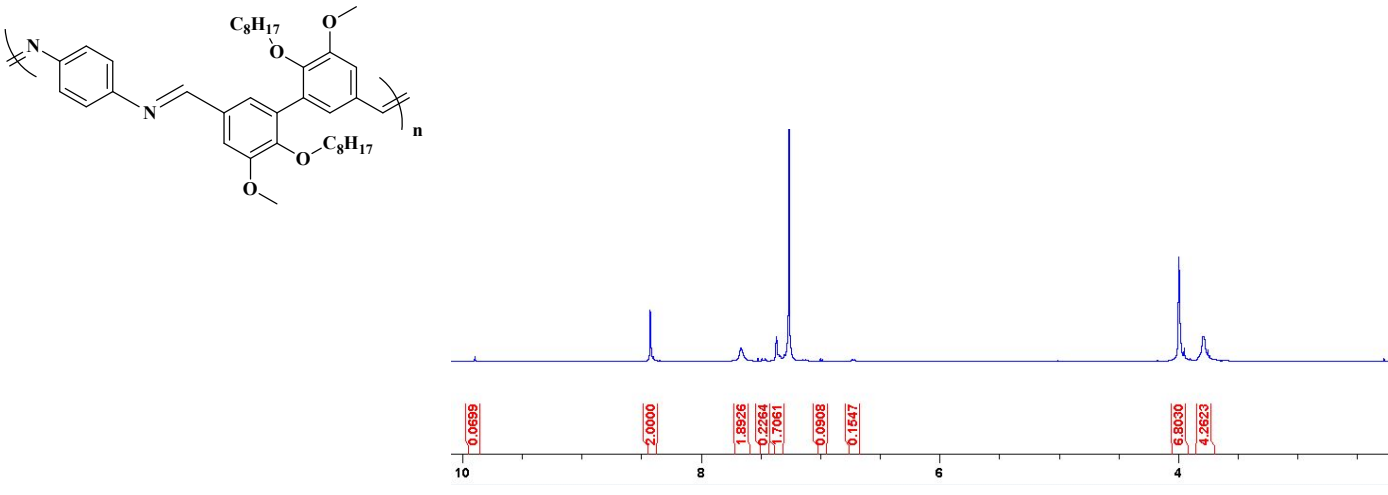


**Figure S5.** $^{1}$H-NMR spectrum of **P1A** (400.20 MHz, in $CDCl_3$)

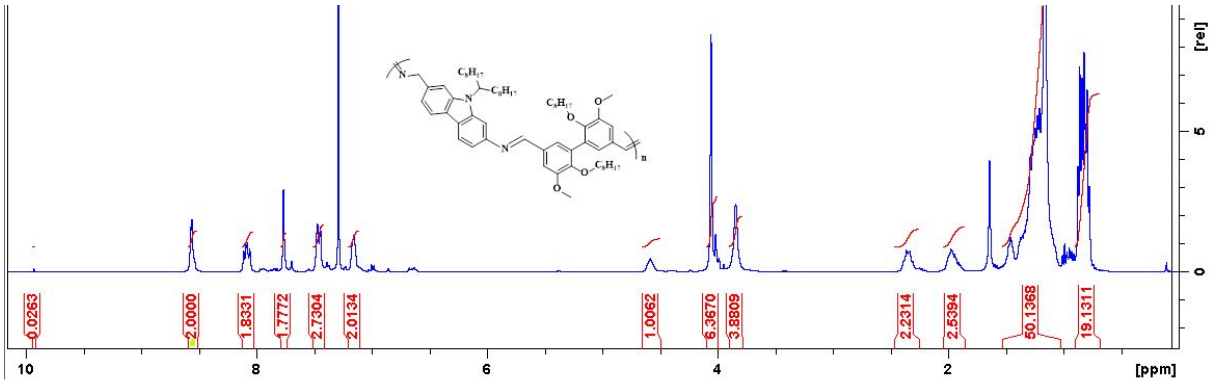


**Figure S6.** $^{1}$H-NMR spectrum of **P2** (400.20 MHz, in $CDCl_3$)

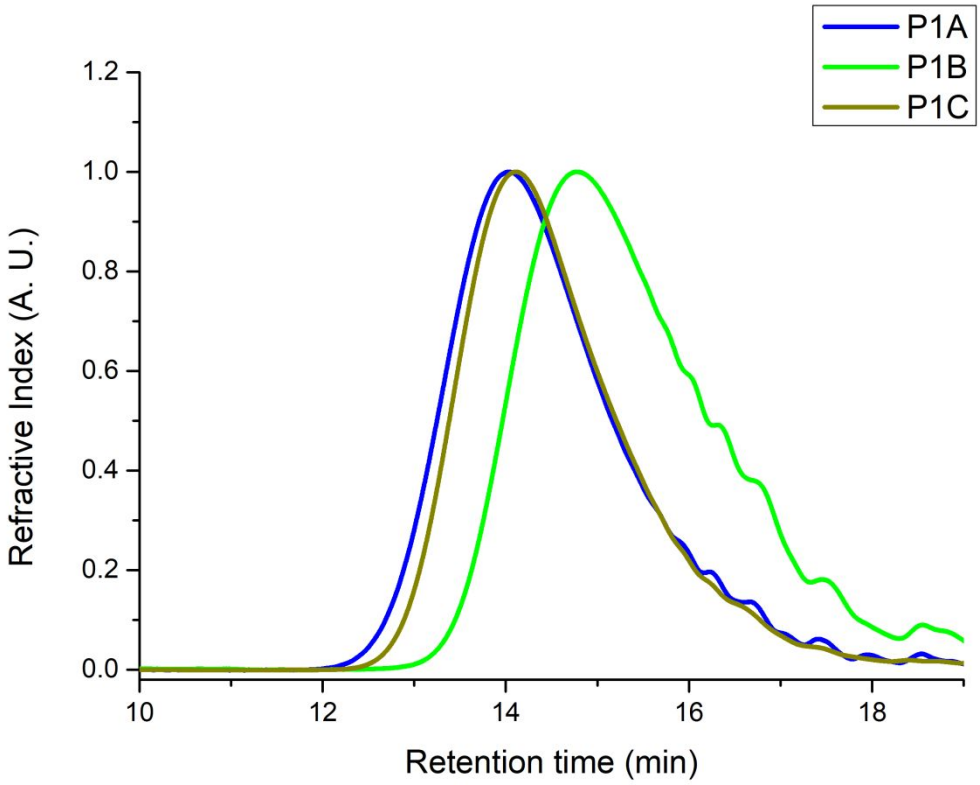


**Figure S7.** SEC traces of **P1A**, **P1B** and **P1C** (in THF, polystyrene standard)

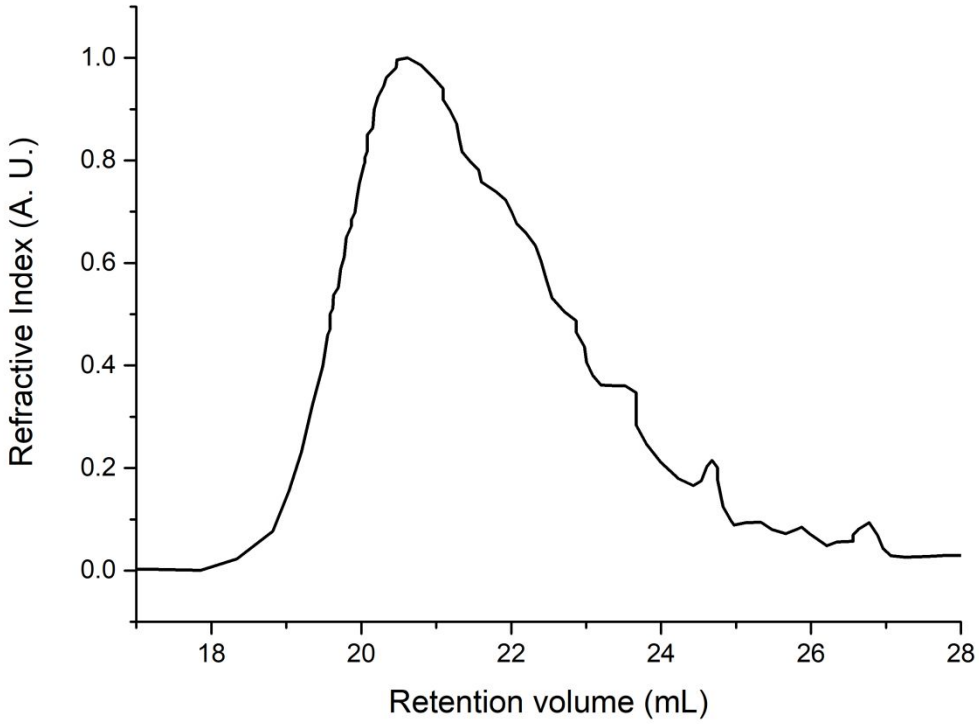


**Figure S8.** SEC trace of **P2** (in THF, polystyrene standard)

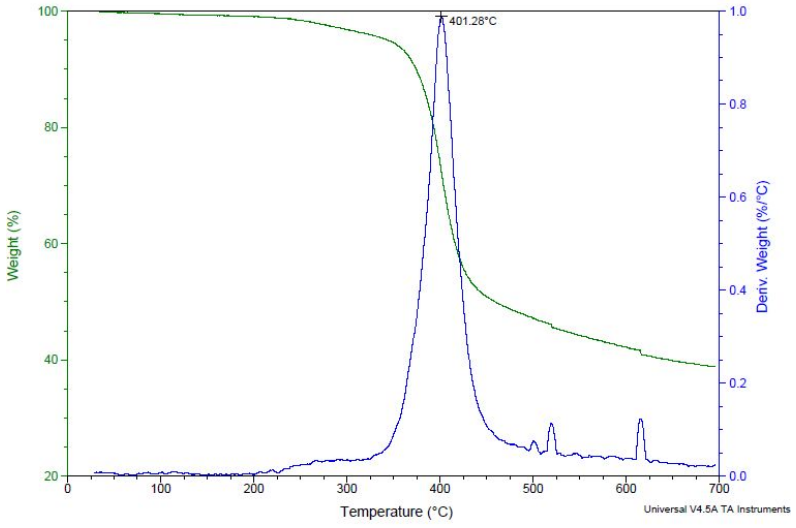


**Figure S9.** TGA trace of **P1A**

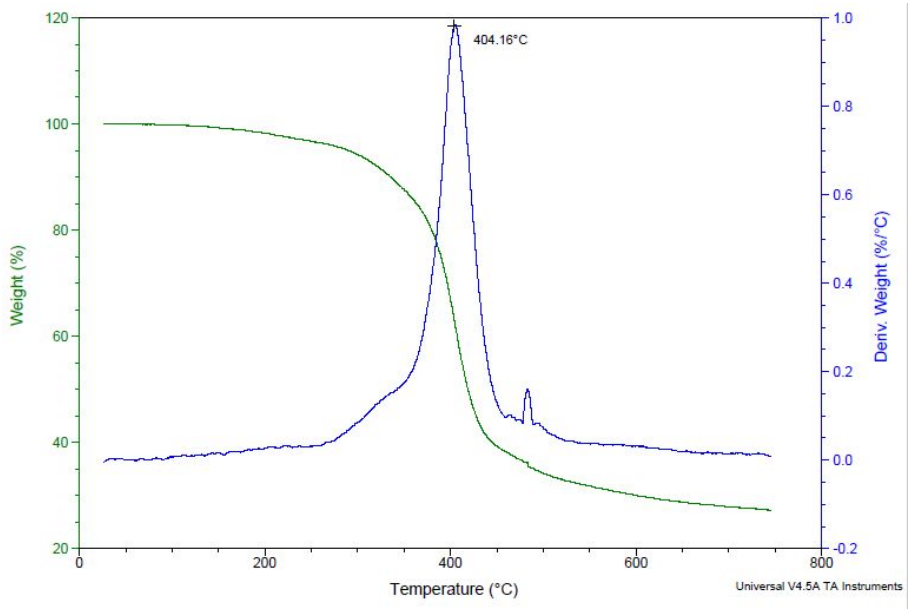


**Figure S10.** TGA trace of **P2**

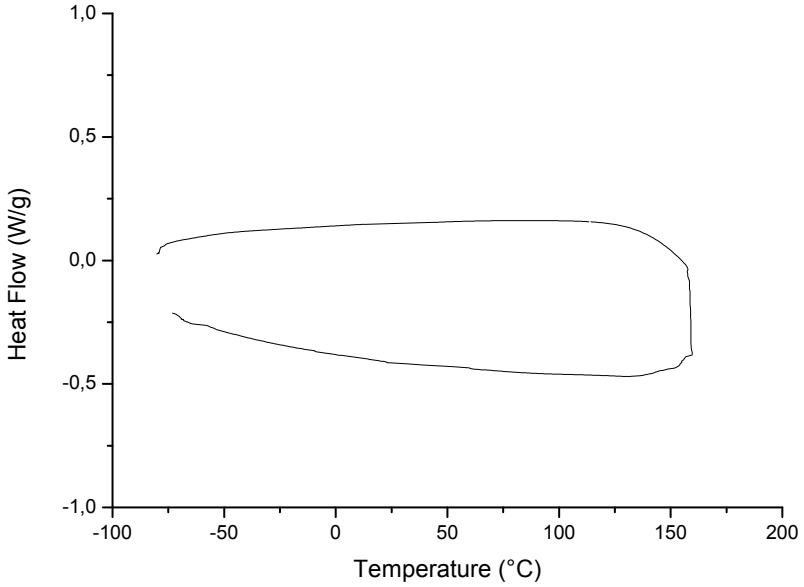


**Figure S11.** DSC trace of **P1A**

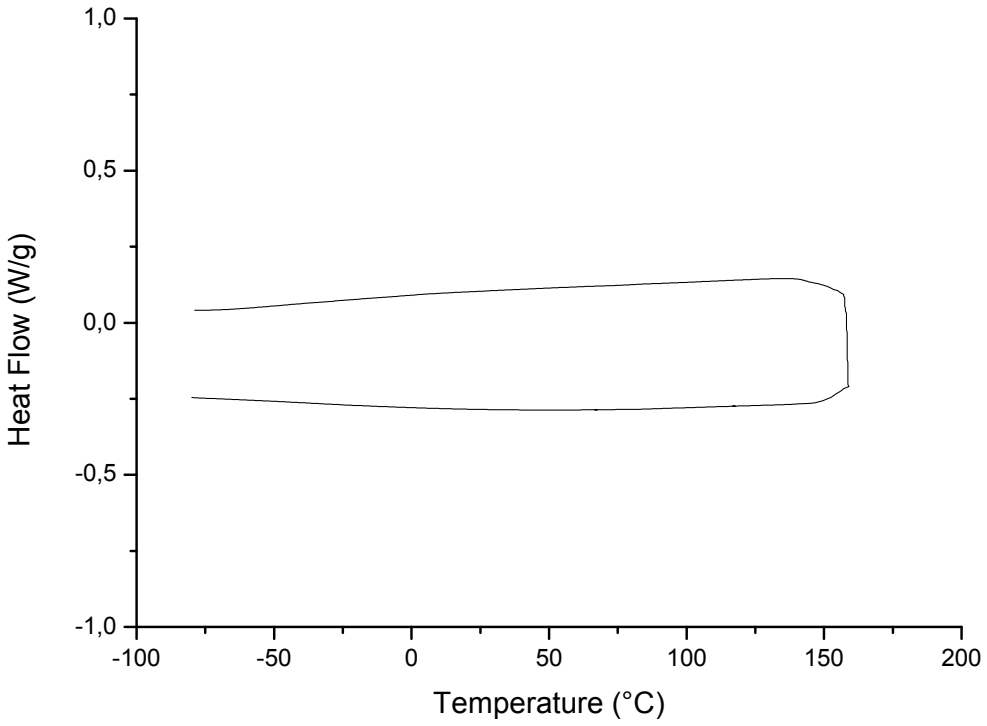


**Figure S12.** DSC trace of **P2**

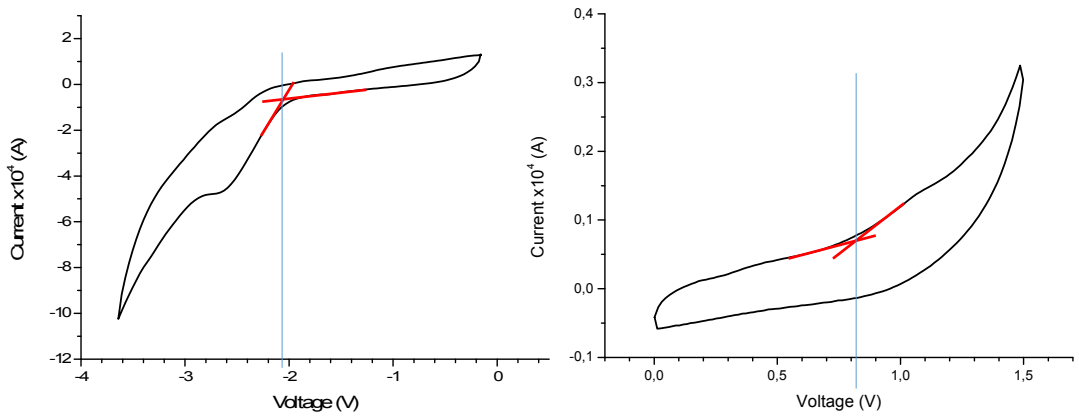


**Figure S13.** Cyclic voltammograms (left-reduction, right-oxidation) of **P1A** in $CH_2Cl_2$ solution

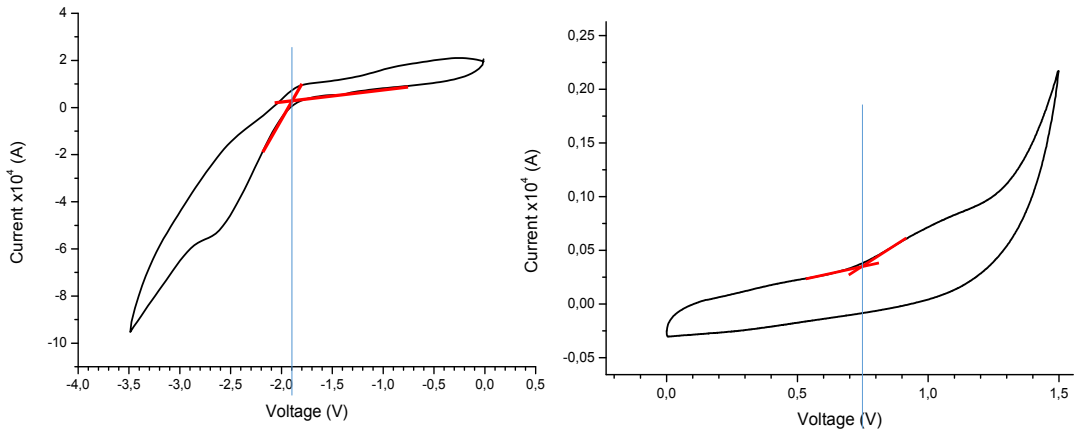


**Figure S14.** Cyclic voltammograms (left-reduction, right-oxidation) of **P2** in $CH_2Cl_2$ solution

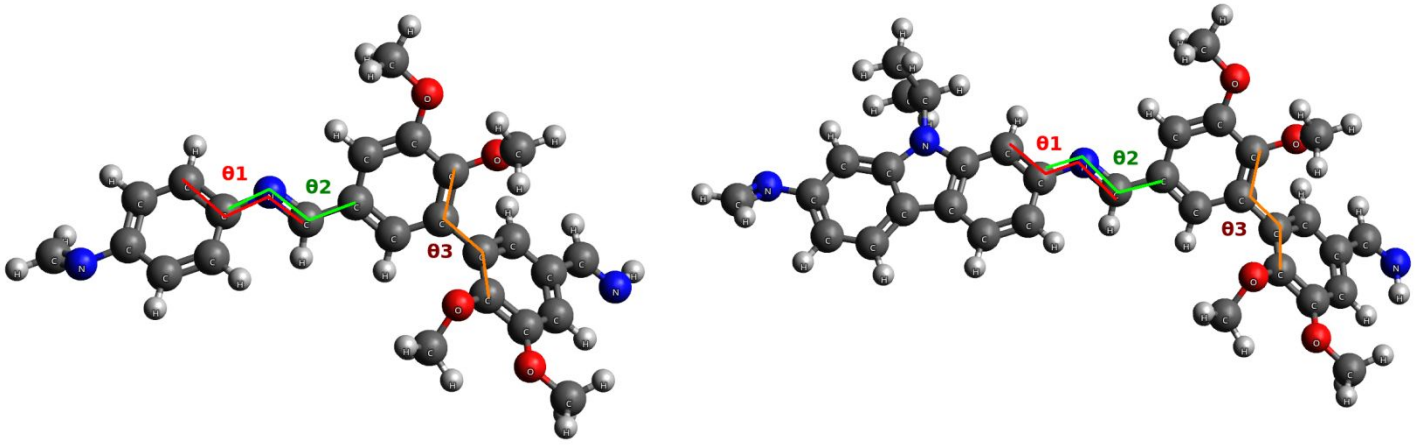


**Figure S15.** Dihedrals considered for the relaxed potential energy surface scans in monomers of (left) **DV-Ph** and (right) **DV-Cbz** derivatives

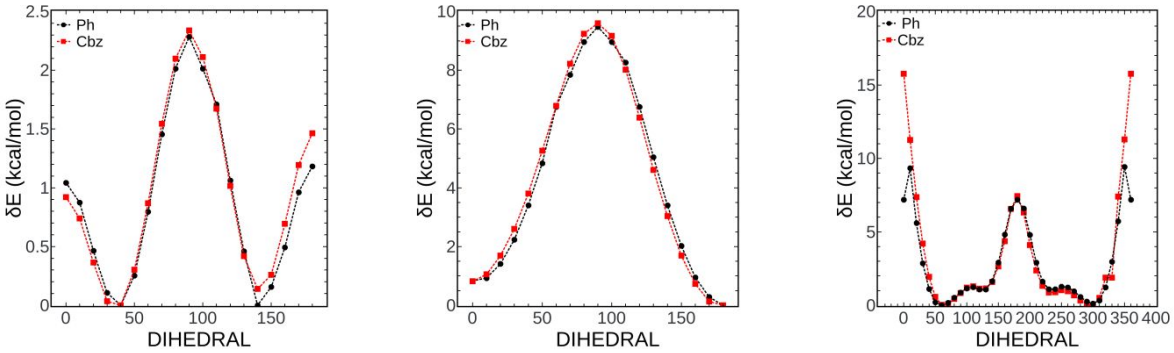


[a] Dihedral: $\theta_1$ [b] Dihedral: $\theta_2$ [c] Dihedral: $\theta_3$

**Figure S16.** Relaxed potential energy surface scans with respect to dihedrals $\theta_1$, $\theta_2$and $\theta_3$ for monomers of **DV-Ph** (Ph: Black - Circles) and **DV-Cbz** (Cbz: Red - Squares)

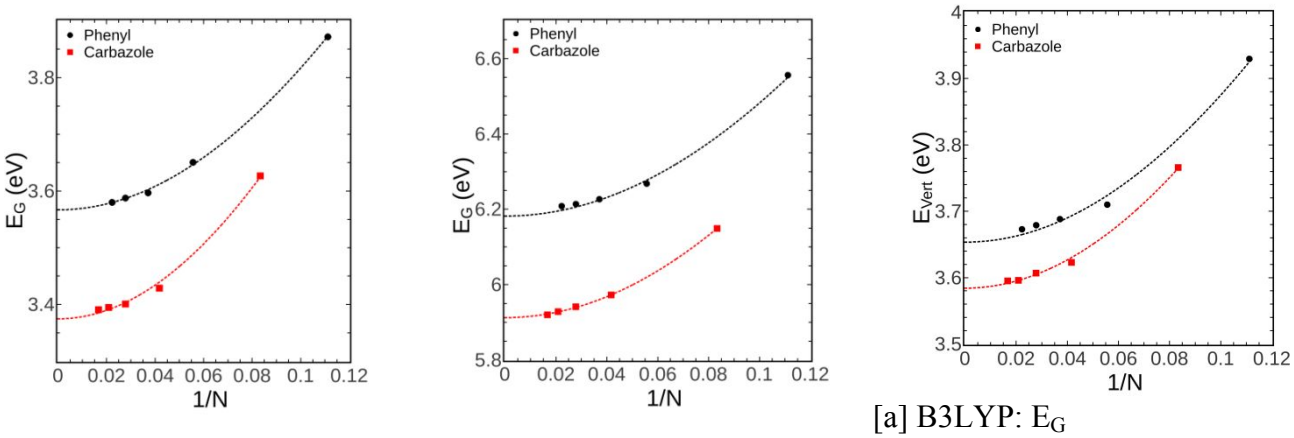


[a] B3LYP: $E_G$

[b] CAM-B3LYP: $E_G$ [c] CAM-B3LYP: $E_{Vert}$

**Figure S17.** Evolution with chain length of the electronic gap of increasing-size **DV-Cbz** (red) and **DV-Ph** (black) oligomers, as calculated at the (a, left) B3LYP/6-31G(d) and (b, centre) CAM-B3LYP/6-31G(c) levels. The right panel reports the evolution of the vertical transition energy ($E_{Vert}$) calculated at the CAM-B3LYP/6-31G (c) level. Dotted lines are Khun fits

| Derivative / Dihedral | $\theta_1$ | $\theta_2$ | $\theta_3$ | ΔE (kcal/mol) |
|---|---|---|---|---|
| **DV-Ph** | 40.0 | 177.48 | 126.39 | 1.020 |
| | 140.0 | 177.53 | 126.31 | 1.149 |
| | 39.55 | 0.0 | 126.51 | 1.864 |
| | 39.89 | 180.0 | 126.84 | 1.036 |
| | **40.08** | **176.98** | **60.0** | **0.0** |
| | 39.73 | 176.96 | 120.0 | 1.072 |
| | | | | |
| **DV-Cbz** | 40.0 | 177.61 | 126.27 | 0.937 |
| | 140.0 | 176.77 | 125.32 | 0.937 |
| | 40.81 | 0.0 | 126.67 | 1.081 |
| | 41.11 | 180.0 | 125.18 | 1.895 |
| | **39.30** | **177.69** | **60.0** | **0.0** |
| | 40.18 | 176.59 | 120.0 | 1.098 |

**Table S1.** Stable conformers obtained from the PES scans for $\theta_1$, $\theta_2$ and $\theta_3$ and relative energies (ΔE in kcal/mol)

| Functional | **DV-Ph** | | | | | **DV-Cbz** | | | | | $\Delta E_{(Phnl-Crbz)}$ | |
|---|---|---|---|---|---|---|---|---|---|---|---|---|
| | HOMO | LUMO | $E_G$ | $\lambda_{max}$ | $E_{Vert}$ | HOMO | LUMO | $E_G$ | $\lambda_{max}$ | $E_{Vert}$ | $\Delta E_G$ | $\Delta E_{Vert}$ |

| | | | | | | | | | | | | |
|---|---|---|---|---|---|---|---|---|---|---|---|---|
| PBE0 | -5.952 | -1.643 | 4.309 | 352 | 3.516 | -5.631 | -1.622 | 4.009 | 376 | 3.294 | 0.300 | 0.222 |
| B3LYP | -5.625 | -1.753 | 3.872 | 394 | 3.375 | -5.329 | -1.702 | 3.627 | 394 | 3.104 | 0.245 | 0.235 |
| CAM-B3LYP | -7.037 | -0.480 | 6.556 | 315 | 3.930 | -6.632 | -0.483 | 6.149 | 329 | 3.766 | 0.407 | 0.164 |
| wB97XD | -7.599 | -0.051 | 7.548 | 313 | 3.951 | -7.220 | -0.065 | 7.155 | 323 | 3.834 | 0.393 | 0.117 |
| M06HF | -8.797 | -0.446 | 8.350 | 301 | 4.107 | -8.286 | -0.353 | 7.933 | 304 | 4.071 | 0.417 | 0.036 |
| M062X | -6.964 | -0.827 | 6.137 | 319 | 3.886 | -6.597 | -0.861 | 5.736 | 333 | 3.716 | 0.401 | 0.170 |

**Table S2.** Electronic ($E_G$) and optical ($E_{Vert}$) gaps (in eV), as well as maximum absorption wavelengths (in nm) of **DV-Cbz** and **DV-Ph** derivatives calculated at the TD-DFT level using various XCFs with the 6-31(d,p) basis set. $\Delta E_{(Phnl\text{-}Crbz)}$ corresponds to differences between the electronic/optical gaps of the two derivatives

| Functional | Unit | DV-Cbz | | | DV-Cbz | | | $\Delta E_{G(Phnl\text{-}Crbz)}$ |
|---|---|---|---|---|---|---|---|---|
| | | HOMO | LUMO | $E_G$ | HOMO | LUMO | $E_G$ | $\Delta E_G$ |
| [a] B3LYP | Monomer | -5.625 | -1.753 | 3.872 | -5.329 | -1.702 | 3.627 | 0.245 |
| | Dimer | -5.516 | -1.894 | 3.621 | -5.224 | -1.795 | 3.429 | 0.192 |
| | Trimer | -5.507 | -1.909 | 3.597 | -5.214 | -1.803 | 3.411 | 0.186 |
| | Tetramer | -5.500 | -1.911 | 3.588 | -5.203 | -1.808 | 3.395 | 0.190 |

| Functional | Unit | **DV-Ph** | | | | | **DV-Cbz** | | | | | $\Delta E_{G(Phnl\text{-}Crbz)}$ | |
|---|---|---|---|---|---|---|---|---|---|---|---|---|---|
| | | HOMO | LUMO | $E_G$ | $\lambda_{max}$ | $E_{Vert}$ | HOMO | LUMO | $E_G$ | $\lambda_{max}$ | $E_{Vert}$ | $\Delta E_G$ | $\Delta E_{Vert}$ |
| [b] CAM-B3LYP | Monomer | -7.037 | -0.480 | 6.556 | 315 | 3.930 | -6.632 | -0.483 | 6.149 | 329 | 3.766 | 0.407 | 0.164 |
| | Dimer | -6.879 | -0.623 | 6.248 | 334 | 3.712 | -6.553 | -0.580 | 5.973 | 342 | 3.623 | 0.275 | 0.089 |
| | Trimer | -6.862 | -0.634 | 6.227 | 336 | 3.688 | -6.535 | -0.594 | 5.941 | 343 | 3.607 | 0.286 | 0.081 |
| | Tetramer | -6.857 | -0.642 | 6.210 | 337 | 3.679 | -6.529 | -0.601 | 5.928 | 344 | 3.596 | 0.285 | 0.083 |

**Table S3.** Electronic ($E_G$) and optical ($E_{Vert}$) gaps (in eV), as well as maximum absorption wavelengths (in nm) of increasing-size **DV-Cbz** and **DV-Ph** derivatives, as calculated at the [a] B3LYP/6-31G(d) and [b] CAM-B3LYP/6-31G(d) levels. $\Delta E_{(Phnl\text{-}Crbz)}$ corresponds to differences between the electronic/optical gaps of the two derivatives

| Derivative / Functional | **DV-Cbz** | | | **DV-Ph** | | |
|---|---|---|---|---|---|---|
| | $E_g$ | $E_0$ | $D_k$ | $E_g$ | $E_0$ | $D_k$ |
| B3LYP | 3.390 | 7.923 | 0.818 | 3.580 | 7.105 | 0.715 |
| CAM-B3LYP | 5.920 | 10.90 | 0.748 | 6.210 | 10.76 | 0.668 |

**Table S4.** Electronic band gap and vertical transition energies at the polymer limit ($E_g$ in eV), and optimized $E_0$ and $D_k$ parameters (in eV, extracted from Equation 1) for **DV-Cbz** and **DV-Ph** derivatives.